Domain Requirement for the Membrane Trafficking and Targeting of Syntaxin 1A*

Xiaofei Yang[‡§1], **Pingyong Xu**[‡§1,2], **Yang Xiao**[‡§], **Xiong Xiong**[‡§], and **Tao Xu**[‡§3]

From the ‡Joint Laboratory of Institute of Biophysics & Huazhong University of Science and Technology, School of Life Science and Technology, Huazhong University of Science and Technology, Wuhan 430074, and the §National Laboratory of Biomacromolecules, Institute of Biophysics, Chinese Academy of Sciences, Beijing 100101, China

Syntaxin plays a key role in intracellular membrane fusion in eukaryotic cells. The function of syntaxin relies on its proper trafficking to and targeting at the target membrane. The mechanisms underlying the trafficking and targeting of syntaxin to its physiological sites remain poorly understood. Here we have analyzed the trafficking of syntaxin 1A in INS-1 and CHO cells. We have identified the transmembrane domain together with several flanking positive-charged amino acids as the minimal domain required for the membrane delivery. Interestingly, we found that SNARE motif-exposed syntaxin 1A mutants were retained in endoplasmic reticulum (ER) and failed to transport to the cell surface in the absence of SNAP-25, suggesting that the exposure of the SNARE motif causes ER retention and complexation with SNAP-25 helps the ER escape. Finally, our data propose two key roles for the H_{abc} domain: to protect nonspecific interaction by masking the SNARE motif and to participate in the clustering of syntaxin 1A to the fusion sites in the plasma membrane.

SNARE[4] (soluble *N*-ethylmaleimide-sensitive factor attachment protein receptor) proteins play a central role in the process of intracellular membrane fusion in eukaryotic cells (for recent reviews, see Refs. 1–3). Intracellular SNAREs can be divided into two categories: the v-SNAREs located on carrier vesicles and the t-SNAREs present on target compartments (4, 5). The interaction between SNAREs present on two opposing membranes is generally believed to provide the driving force to initiate membrane fusion. Syntaxin 1A (Stx1A) is a t-SNARE predominantly located at the plasma membrane and has been shown to be essential for vesicle fusion (6). The essential requirement of Stx1A for exocytosis has been demonstrated in that deletion of its homologues leads to complete loss of synaptic transmission in *Drosophila* (7) and complete paralysis in *Caenorhabditis elegans* (8).

To function appropriately, the SNAREs themselves must be correctly sorted and delivered to destination compartments. The intracellular trafficking of t-SNARE syntaxin is particularly intriguing as syntaxin belongs to a family of proteins that are "tail-anchored," also called Type IV membrane proteins (9). Such proteins have an N-terminal cytoplasmic domain that is membrane-bound by virtue of a single C-terminal hydrophobic domain. These proteins lack an N-terminal signal sequence, and their membrane-interacting region is so close to the C terminus that it emerges from the ribosome only upon termination of translation. The trafficking and targeting mechanism of these tail-anchored proteins have largely remained obscure.

The trafficking of syntaxin may require the interaction with "accessory" proteins. For instance, it has been demonstrated that neural specific Stx1A sorting from the Golgi complex and delivery to the plasma membrane required Munc18-1 (10). However, this hypothesis has been challenged by another research demonstrating that syntaxin transportation to the membrane is independent of unc18 protein in *C. elegans* (11). A recent research in *munc18-1* knock-out mice also showed that Munc18-1 is not essential for Stx1A delivery to the presynaptic terminal (12).

To gain further insight into the mechanism of Stx1A trafficking and the functional construction of the protein, we have recently investigated the subcellular localization of Stx1A in INS-1 and CHO cells. The intracellular trafficking and distribution of Stx1A have not been characterized in these cells. These two cell types were selected because INS-1 cells are insulin-secreting cells that express endogenously Stx1A, Munc18-1, and SNAP-25 (13, 14), whereas we verified that non-secretory CHO cells possess no endogenous Stx1A and Munc18-1 (data not shown). CHO cells hence serve as a good model to study the dependence of Stx1A trafficking on Munc18-1. Herein we have quantitatively studied the trafficking of wild type Stx1A and its truncation mutants in both INS-1 and CHO cells employing a pH-sensitive fluorescent protein label, pHluorin. We have identified the molecular determinants of the trafficking and targeting of Stx1A.

EXPERIMENTAL PROCEDURES

Materials—Mouse anti-Stx1A monoclonal antibodies were from Sigma. Restriction enzymes and other standard molecular biology reagents were from New England Biolabs (Ipswich, MA). Chemicals were from Sigma or as indicated in the text. The ER marker pDsRed2-ER and the Golgi marker pEYFP-Golgi were from Clontech Laboratories.

DNA Construction—Expression plasmids encoding pHluorin-fused wild type Stx1A (Stx1A-pHluorin) and truncated recombinant (t1–t8) were constructed by cloning Stx1A cDNA (15) and pHluorin cDNA (16) into pcDNA3.1Zeo(+) vector (Invitrogen). Plasmid SNAP-25-TDimer2 was constructed as described previously (17). For construction of mRFP-IRES-BoNT/E, mRFP (18) was first amplified and cloned into pIRES vector (Clontech Laboratories), and then botulinum neurotoxin type E (BoNT/E) (19) was ligated into the subclone vector. To generate a red fluorescence

protein-targeted Golgi marker, pmSrawberry-Golgi, the red fluorescence protein mStrawberry (20) was used to substitute EYFP in pEYFP-Golgi. For construction of Munc18-1-TDimer2 fusion construct, the Munc18-1 PCR fragment was ligated into subclone vector pcDNA3.1-TDimer2 (17). Construct integrity was verified using DNA sequencing analysis provided by Invitrogen Biotechnology (Beijing, China). H_{abc} fragment was amplified with PCR and cloned into pIRES-EGFP vector (Clontech Laboratories), and then EGFP was substituted with mRFP.

Cell Culture—CHO cells were grown at 37 °C in complete medium: Iscove's modified Dulbecco's medium/F-12 medium (Invitrogen) supplemented with 10% fetal bovine serum (Invitrogen), 2 mM L-glutamine (pH 7.4). INS-1 cells were cultured as described previously (21). Briefly, cell cultures were maintained in RPMI 1640 culture medium containing 10 mM Hepes, 11.1 mM glucose, 10% fetal bovine serum, 100 units/ml penicillin G, 100 μg/ml streptomycin, 2.0 mM L-glutamine, 1.0 mM sodium pyruvate, and 50 μM 2-mercaptoethanol.

Transfection—INS-1 or CHO cells were transfected with Lipofectamine™ 2000 transfection reagent (Invitrogen) as per the manufacturer's recommendations. The day prior to the experiment, cells were transferred onto a poly-L-lysine-coated round coverslip at a density of 50,000 cells per chamber.

Antibodies and Western Blotting—Cell extracts were prepared by washing the cells with phosphate-buffered saline and then extracting proteins with lysis buffer (in mM): 10 Tris, 3 $CaCl_2$, 2 $MgCl_2$, 2.5% Nonidet P-40 (pH 7.5). Protein concentration was determined with the Pierce BCA protein reagent kit (Pierce). Samples were resolved by SDS-PAGE and analyzed by standard Western blotting techniques. Anti-Munc18-1 polyclone anitibody (1:3000) was from BD Biosciences and anti-β-actin monoclonal antibody (1:5000) was from Sigma.

RNA Interference—To generate a red fluorescence protein-labeled shRNA vector, mRFP (20) was used to substitute cGFP in pRNAT-H1.1/Neo (GenScript Corp., Piscataway, NJ). Small hairpin oligonucleotides (shRNA) to suppress Munc18-1 expression were designed according to the recommendations given by Miyagishi *et al.* (22) and cloned into the BamHI-HindIII sites of the vector pRNAT-H1.1/RFP. Oligonucleotide sequences with the highest knockdown efficiency were as follows: sense, 5′-gat ccg cgt tac taa ggt act gta ttc aag aga tac ggt gcc ttg gta atg ctt ttt tgg aaa-3′; antisense, 5′-agc ttt tcc aaa aaa gca tta cca agg cac cgt atc tct tga ata cag tac ctt agt aac gcg-3′.

Fluorescence Imaging—Cells were viewed under Olympus confocal laser scanning biological microscope FV500 with 60 × (NA = 1.40) oil objective after transfection. pHluorin fluorescence was excited by 488 nm argon laser, and TDimer2 (or mStrawberry) fluorescence was excited by a 543 nm HeNe laser (Melles Griot). Images were acquired and analyzed using FLUOVIEW (Olympus Optical Co., Tokyo, Japan) and Photoshop 6.0.

Total internal reflection fluorescence microscopy (TIRFM) setup was constructed based on the prismless and through-the-lens configuration using the TIRF condensor made from TILL (TILL Photonics, Gräfelfing, Germany). The GFP and RFP fluorescence were both excited by a 488 nm argon laser. To image the green and the red fluorescence simultaneously, a dual-View Micro-Imager (Optical-Insights, Santa Fe, NM) was inserted before the cooled CCD (PCO Electron Multiplying CCD, PCO Computer Optics, Kelheim, Germany). Images were collected, corrected for background, processed, and analyzed using TILLvisION4.01 (TILL Photonics).

Calculation of Surface Fraction and pH of the Intracellular Compartment—We designed experiments to quantify the relative amount of Stx1A-pHluorin on the cell surface compared with that in the cytosol. INS-1 and CHO cells were first incubated in the non-permeating normal solution (pH 7.4) after 48-h transfection. The external solution was then
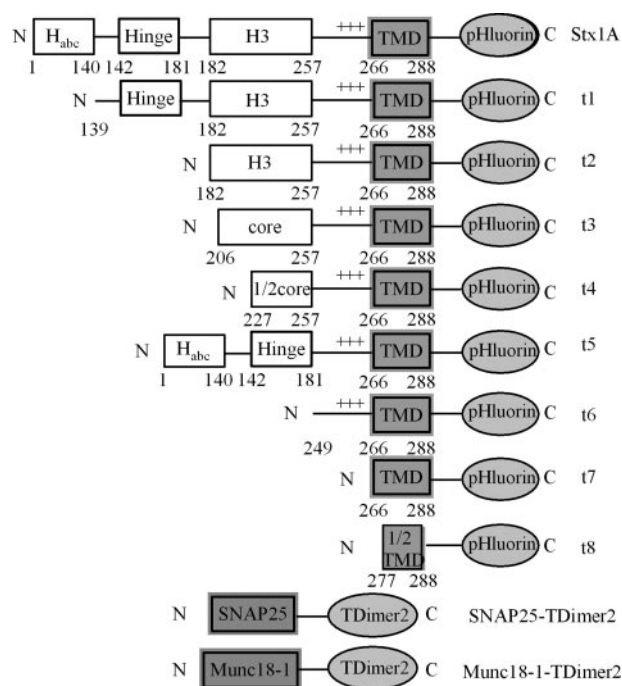
FIGURE 1. **A schematic representation of the constructs used in this study.** *Left* and *right sides* are the N and C termini, respectively. pHluorin was fused to the C termini of each Stx1A mutant. SNAP-25 and Munc18-1 were fused with TDimer2 at the C terminus. The length in amino acids of each region is indicated.

changed in turn to non-permeating pH 5.5 solution, permeating pH 7.4 NH_4Cl solution, and normal wash solution. The surface fraction of Stx1A-pHluorin and the pH of the intracellular compartment (pH_i) were determined as described previously (23). Briefly, during application of a pH 5.5 solution, we define $f(pH_i)$ as surface fraction of Stx1A-pHluorin as a function of internal pH_i,

$$f(\mathrm{pH}_i) = \frac{\epsilon}{1 - \phi(\mathrm{pH}_i) + \alpha(\mathrm{pH}_i)(1 - \epsilon)} \quad \text{(Eq. 1)}$$

where $\alpha(\mathrm{pH}_i) = (1/(1 + 10^{pK-7.4}) - 1/(1 + 10^{pK-\mathrm{pH}_i}))/(1/(1 + 10^{pK-\mathrm{pH}_i}))$, $\phi(\mathrm{pH}_i) = (1/(1 + 10^{pK-5.5}))/(1/(1 + 10^{pK-\mathrm{pH}_i}))$, and ϵ is a mean value for the fractional increase in fluorescence during application of a non-permeating pH 5.5 solution. The pK of pHluorin was set to 7.07 as determined previously (24).

During application of NH_4Cl solution, the surface fraction of Stx1A-pHluorin, $f(pH_i)$, can be calculated as follows,

$$f(\mathrm{pH}_i) = \frac{\alpha(\mathrm{pH}_i) - \gamma}{\alpha(\mathrm{pH}_i)\gamma + \alpha(\mathrm{pH}_i)} \quad \text{(Eq. 2)}$$

where γ is the mean value for the fractional increase in fluorescence during application of NH_4Cl solution at pH 7.4.

The functions for $f(pH_i)$ derived from Equations 1 and 2 as described above were plotted to estimate the pH of the intracellular compartment. The point of intersection gave us a readout of mean intracellular pH, and the surface fraction of Stx1A-pHluorin was calculated by using the mean pH value (23).

RESULTS

Stx1A Is Delivered to the Plasma Membrane in Both INS-1 and CHO Cells—To examine the roles of different domains in Stx1A trafficking and localization, we have generated series deletion mutants of Stx1A as shown in Fig. 1. To investigate the intracellular distribution of these
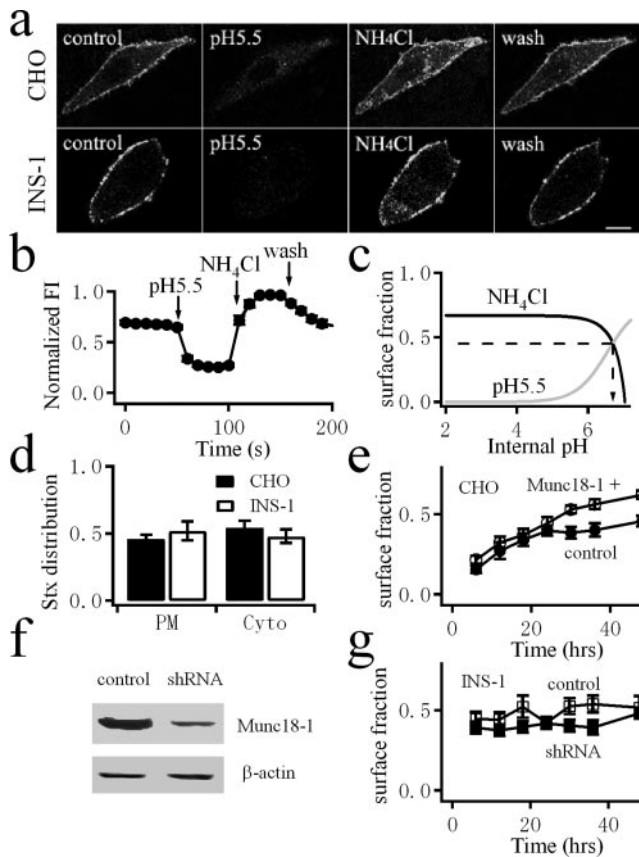
FIGURE 2. **Quantitative analysis of cell surface Stx1A using pHluorin.** *a*, confocal images of Stx1A-pHluorin in different extracellular solutions from CHO and INS-1 cells. Application of external solution at pH 5.5 quenched cell surface pHluorin, and application of NH_4Cl solution at pH 7.4 brightened up the intracellular fluorescence of pHluorin. *Bar*, 5 μm. *b*, effects of pH 5.5 and NH_4Cl solution on the normalized fluorescence intensity (*Fl*) of pHluorin. The overall cell fluorescence after background subtraction was normalized to the steady-state fluorescence in the NH_4Cl solution. *Arrows* indicate change of solution. *c*, surface fraction of Stx1A-pHluorin as a function of pH of internal compartment calculated from acid quenching data (pH 5.5; *gray line*) or NH_4Cl data (*dark line*) according to Equations 1 and 2, respectively (23). The *arrow* indicates the pH value at which the curves intersect. *d*, averaged content of Stx1A-pHluorin in the plasma membrane and cytosol from CHO (*solid bar*) and INS-1 (*open bar*) cells. *e*, dynamic change of surface fraction of Stx1A-pHluorin in control CHO cells (*filled symbols*) and cells overexpressed with Munc18-1 (*open symbols*). *f*, Western analysis comparing Munc18-1 protein levels between control INS-1 cells and cells transfected with shRNA against Munc18-1. *g*, dynamic change of surface fraction of Stx1A-pHluorin in control INS-1 cells (*open boxes*) and cells transfected with shRNA against Munc18-1 (*filled boxes*).

mutants and wild type Stx1A in living cells, we tagged these proteins at its C terminus with the pH-sensitive GFP variant, ecliptic pHluorin. Ecliptic pHluorin is brightly fluorescent at pH 7.4 but almost non-fluorescent at about pH < 6.0 (16). pHluorin at the C terminus of Stx1A mutants will be embedded in the lumen of intracellular compartments and will be exposed extracellularly when inserted into the plasma membrane. Thus, pHluorin is a good marker to study the cell surface localization of Stx1A, which is usually not easy when GFP is used. In addition, one can quantify the surface fraction of pHluorin-labeled proteins by comparing the fluorescence changes between surface quenching using acidic extracellular solution (pH 5.5) and dequenching internal pHluorin with membrane-permeant NH_4Cl solution (pH 7.4), as described previously (23). We first examined the subcellular localization of exogenous expressed Stx1A-pHluorin in CHO cells by laser scanning confocal microscopy. We verified that there is no endogenous Stx1A expressed in CHO cells (data not shown). As shown in Fig. 2*a*, Stx1A-pHluorin fluorescence was mainly observed at the peripheral boundary of the cell, with some distribution inside the cell. The rim-like peripheral

distribution represents cell surface Stx1A-pHluorin because it is largely quenched upon extracellular perfusion of solution at pH5.5 (Fig. 2*a*). Application of NH_4Cl solution buffered at pH 7.4 resulted in an increase in intracellular fluorescence, suggesting that some Stx1A-pHluorin is present at acidic intracellular compartments. INS-1 cells transfected with Stx1A-pHluorin displayed a similar distribution (Fig. 2*a*). As exemplified in Fig. 2*b*, extracellular application of pH 5.5 solution resulted in a significant decrease in the normalized fluorescence, whereas switching to NH_4Cl solution caused an increased fluorescence. By calculating the surface fraction of Stx1A-pHluorin in pH 5.5 and NH_4Cl solutions according to Equations 1 and 2, respectively, we estimated a mean internal pH (pH_i) of 6.6 (Fig. 2*c*), suggesting that intracellular Stx1A-pHluorin resides in acidic compartments. Using this mean pH_i we quantified the surface fraction of Stx1A-pHluorin in both CHO and INS-1 cells. The surface fraction of Stx1A on the plasma membrane 48 h after transfection was 45.9 ± 3.3% (*n* = 16) for CHO cells, similar to that in INS-1 cells (51.9 ± 7.1% *n* = 11, see Fig. 2*d*).

Interestingly, by doing time-course experiments, we found that delivery of Stx1A-pHluorin to the plasma membrane was much slower in CHO cells as compared with INS-1 cells. The surface fraction of Stx1A-pHluorin in CHO cells was rather low at 6 h after transfection and reached a plateau 24 h after transfection, whereas the surface fraction in INS-1 cells remained constant even from 6 h after transfection (Fig. 2, *e* and *g*). The different time course may result from Munc18-1 proteins, which are only expressed in INS-1 cells. To explore the role of Munc18-1 in Stx1A trafficking, we manipulated the level of Munc18-1 and examined the rate and extent of Stx1A surface translocation in both cell types. In CHO cells, which do not express Munc18-1, overexpression of Munc18-1 exerts no significant influence on the surface fraction of Stx1A (Fig. 2*e*). The slight enhancement after 24-h transfection may be explained by the previous finding that Munc-18 can stabilize Stx1A on the plasma membrane (12). Transfection with rat-specific shRNA against Munc18-1 in INS-1 cells reduced the protein level by >85% (Fig. 2*f*). However, no significant difference in Stx1A surface translocation between control and Munc18-1 knockdown cells was observed (Fig. 2*g*). The results suggest that trafficking of Stx1A to the plasma membrane is independent of Munc18-1.

SNAP-25 Interacts with Exposed SNARE Motif of Stx1A and Transports It to the Cell Surface—The cytoplasmic portion of Stx1A consists of two helical domains: H_{abc} and H3 (25). The H_{abc} domain is thought to bind the H3 domain (SNARE motif) in an antiparallel four-helix bundle. The binding of H_{abc} domain to the SNARE motif renders Stx1A in a closed configuration that is essential for the interaction with Munc18-1. To investigate the role of H_{abc} domain in the trafficking of Stx1A, we first generated different N-terminal truncated mutants that preserve the intact SNARE motif, which we designated t1, t2, and t3 here. These SNARE motif-exposed mutants were found localized to the plasma membrane in INS-1 cells (Fig. 3*a*), suggesting that their trafficking does not require Munc18-1. Surprisingly, they failed to translocate to the plasma membrane in CHO cells (Fig. 3*a*). The averaged surface fraction of these mutants in CHO cells were 4.0 ± 1.0% (*n* = 12), 4.7 ± 1.0% (*n* = 12), and 5.4 ± 1.3% (*n* = 12) for t1, t2, and t3, respectively. These values are markedly lower than those in INS-1 cells (compare with Fig. 3*d*). One explanation for the mislocalization of the mutants in CHO cells could be due to the lack of a certain factor to facilitate the transportation of the mutant proteins. We first verified that co-transfection of Munc18-1 in CHO cells does not rescue the trafficking (data not shown). Interestingly, co-transfection of SNAP-25 rescued the membrane localization of all three mutants in CHO cells (Fig. 3*b*, *upper panels*, and Fig. 3*c*). The surface fraction of the t1 mutant was recovered

FIGURE 3. **Distribution and surface fraction of SNARE motif-exposed Stx1A mutants in CHO and INS-1 cells.** *a,* confocal images of expressed t1 mutant of Stx1A from example CHO or INS-1 cell. *b,* confocal images of t1 mutant and co-expressed SNAP-25-Tdimer2. *Bar,* 5 μm. *c* and *d,* averaged surface fraction of the Stx1A mutants (t1, t2, t3) when expressed alone or co-expressed with SNAP-25 (*S*) in either CHO or INS-1 cells.
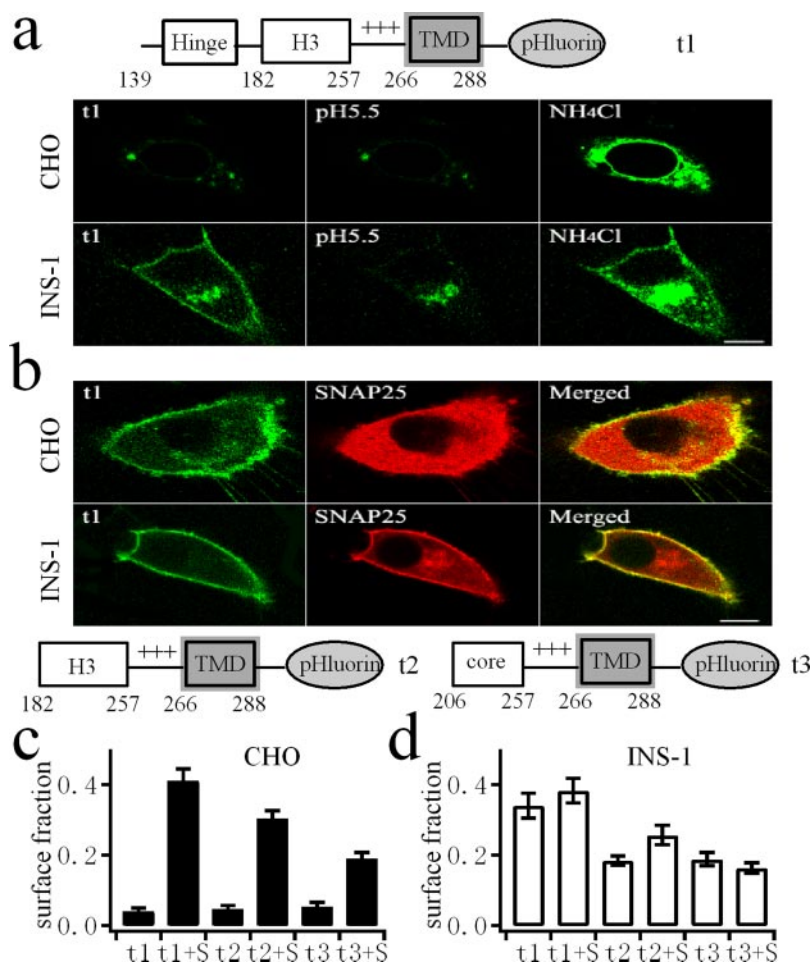
to 41.13 ± 3.36% (*n* = 22) by co-expressed SNAP-25, which is similar to the value for wild type Stx1A in CHO cells. t2 and t3 mutants were less efficiently recovered by SNAP-25, suggesting the hinge region flanking the core SNARE motif of Stx1A participates in stabilizing the interaction with SNAP-25 (Fig. 3*c*). We further determined that SNAP-25 can traffic to the plasma membrane in CHO cells (data not shown), consistent with previous observation that SNAP-25 trafficking is independent of syntaxin (26). In INS-1 cells, co-expression of SNAP-25 with t1–t3 mutants resulted in comparable surface fractions as those from cells without SNAP-25 co-transfection (Fig. 3*d*), probably due to the presence of native SNAP-25 proteins. As we have shown in Fig. 3*b*, co-expressed SNAP-25 and SNARE motif-exposed Stx1A mutants co-localized at the plasma membrane (t1 as an example; t2 and t3 not shown).

To examine at which step the trafficking of the SNARE motif-exposed Stx1A mutants is impaired in CHO cells, we employed ER and Golgi maker tagged with red fluorescence proteins. When co-expressed with pDsRed2-ER or pmSrawberry-Golgi to label ER or Golgi, respectively, the mutants were found to be retained in ER and could not be transported into Golgi network in CHO cells (Fig. 4*a*, t3 as an example). In contrast, besides the cell surface distribution, a substantial amount of the mutant Stx1A proteins co-localized with Golgi maker in INS-1 cells, suggesting these mutants exit ER, enter Glogi network, and then are transported to the plasma membrane (Fig. 4*b*).

The above data suggest that the SNARE motif-exposed mutants may interact with other SNARE motifs inside ER and hence be retained without trafficking to the Golgi and plasma membrane in CHO cells; whereas in INS-1 cells, endogenously expressed SNAP-25 may compete

with the putative ER SNARE(s) for interaction with the exposed SNARE motif of Stx1A. SNAP-25 has been shown to form a high affinity binary complex with Stx1A (27, 28). The complexed Stx1A mutants then can be transported to the plasma membrane via SNAP-25-dependent pathway or its own sorting pathway. To test this hypothesis, INS-1 cells were co-transfected with the light chain of botulinum neurotoxin type E (BoNT/E), a toxin that specifically cleaves SNAP-25 and impairs its interaction with Stx1A (29). After co-expression of BoNT/E in INS-1 cells, the membrane localization of the SNARE motif-exposed Stx1A mutants was almost completely blocked (Fig. 5). As control, the surface delivery of full-length Stx1A was not impaired by BoNT/E treatment (Fig. 5*b*). These results confirm that endogenous SNAP-25 participates in the delivery of the SNARE motif-exposed mutants, but not the complete Stx1A, to the plasma membrane.

If indeed the exposed SNARE motif of Stx1A induces its retention in ER, ablation of the SNARE motif will render membrane delivery of Stx1A. We thus generated a longer N-terminal truncation extending to the middle of the SNARE core motif (t4) or a mutant where only the SNARE core motif is deleted (t5). The subcellular distribution of these mutants were studied when expressed alone or co-expressed with SNAP-25 in CHO and INS-1 cells. Confocal analysis showed that both mutants transported to the cell surface in both cell types (Fig. 6*a*). As shown in Fig. 6*b*, the surface fractions of t4 and t5 reach 46.8 ± 3.6% (*n* = 14) and 46.3 ± 3.7% (*n* = 12) in CHO cells, which is not significantly different from the value for wild type Stx1A (see Fig. 2). The surface fractions of t4 and t5 in INS-1 cells are somewhat lower than that of wild type Stx1A (Fig. 6*c*). Furthermore, the surface fractions of the
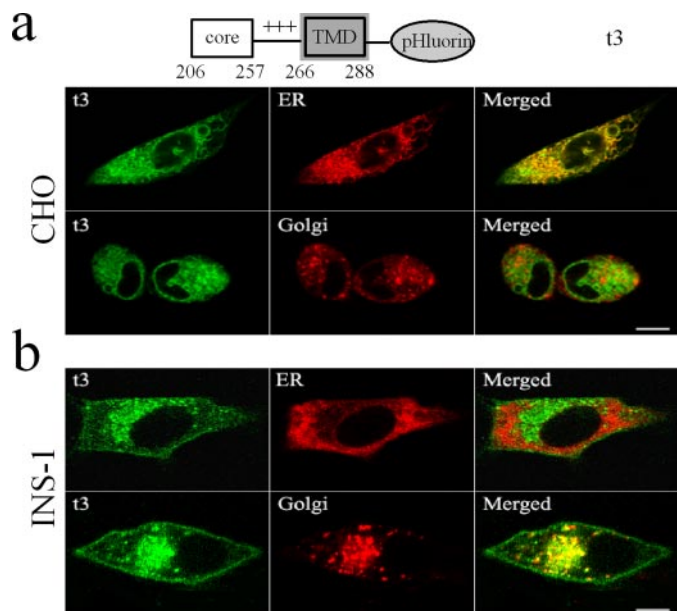
FIGURE 4. **SNARE motif-exposed Stx1A is retained mainly in ER in CHO cells but transports to Golgi and plasma membrane in INS-1 cells.** Confocal images of SNARE motif-exposed Stx1A (t3 as an example) in CHO (*a*) or INS-1 (*b*) cells. *Bar*, 5 μm. Also shown are images of ER or Golgi markers from cells co-transfected with either pDsRed2-ER or pmSrawberry-Golgi. Merged images are shown in the *right column*.
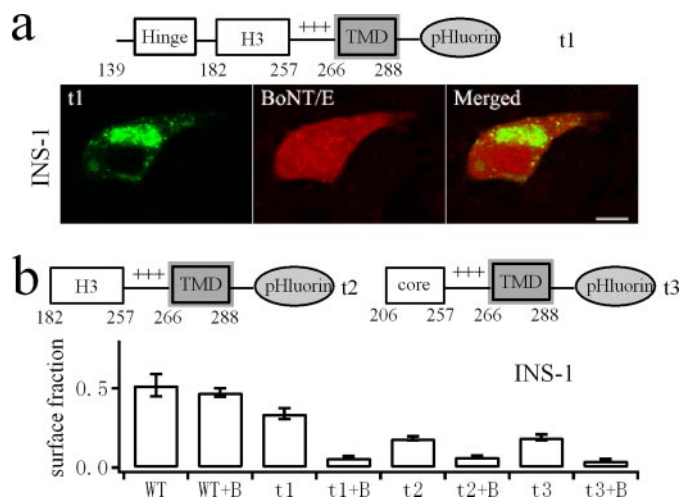

FIGURE 5. **Cleavage of endogenous SNAP-25 by BoNT/E abolishes cell surface localization of SNARE motif-exposed Stx1A mutants in INS-1 cells.** *a*, confocal images of co-expressed SNARE motif-exposed Stx1A mutants (t1 as an example) and cytosolic mRFP (as an indicator of BoNT/E expressed by pmRFP-IRES-BoNT/E vector) in INS-1 cells. *Bar*, 5 μm. *b*, averaged surface fraction of the SNARE motif-exposed mutants (t1, t2, t3) and full-length Stx1A (wild type (*WT*)) when expressed alone or co-expressed with BoNT/E (*B*) in INS-1 cells.

FIGURE 6. **Disruption of SNARE motif in Stx1A enables the delivery of Stx1A mutants (t4 and t5) to cell surface in both CHO and INS-1 cells.** *a*, distribution of t4 and t5 in CHO and INS-1 cells. *Bar*, 5 μm. *b* and *c*, averaged surface fraction of t4 and t5 when expressed alone or co-expressed with SNAP-25 (*S*) in CHO and INS-1 cells. SNAP-25 has no apparent effect on the surface fraction of the two mutants.

FIGURE 7. **Minimal domain required for Stx1A delivery to the plasma membrane.** *a*, confocal images of t6, t7, and t8 mutants in CHO and INS-1 cells. *Bar*, 5 μm. *b*, averaged surface fraction of t6, t7, and t8 mutants in CHO (*solid bars*) and INS-1 (*open bars*) cells.

two mutants were not significantly influenced by co-expression of SNAP-25 (Fig. 6, *b* and *c*). These results further support our hypothesis that it is the exposed SNARE motif that causes the ER retention.

Minimal Domain Requirement of Stx1A for Plasma Membrane Localization—To identify the minimal domain required for the trafficking of Stx1A, we started from t4 and made shorter truncations (t6–t8). By chopping half of the transmembrane domain (TMD), t8 exhibited a homogenous cytosolic distribution in both INS-1 and CHO cells (Fig. 7*a*). The t7 mutant that preserves the intact TMD displayed a diffusible distribution that resembles the distribution of ER. Neither t7 nor t8 transported to the plasma membrane as assessed by the calculated surface fractions in Fig. 7*b*. Interestingly, when the positively charged residues flanking the TMD were included in t6, we found distinctive
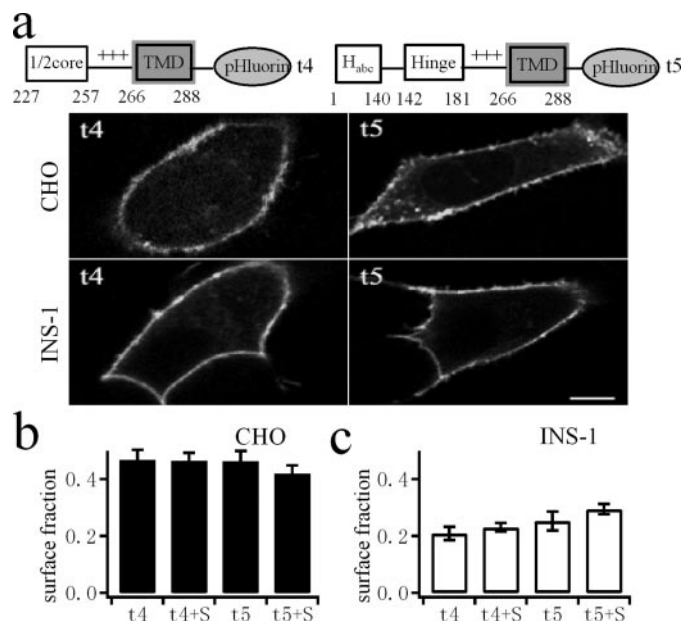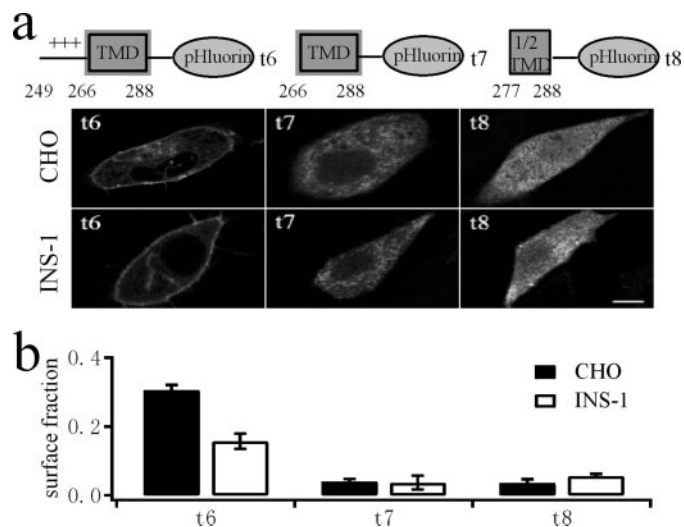
plasma membrane localization (Fig. 7*a*) and a significant level on the cell surface (Fig. 7*b*). We thus propose that residues 249–288 constitute the minimal sequence for the trafficking of Stx1A to the plasma membrane. The positively charged residues flanking the TMD likely stabilize Stx1A on the membrane through the interaction with negatively charged lipid.

The Role of H_{abc} Domain in Stx1A Trafficking and Clustering—After insertion into the plasma membrane, there probably exists a further process for targeting Stx1A to its sites of action. It has been reported that Stx1A is concentrated in cholesterol-dependent clusters that define docking and fusion sites for exocytosis in cracked PC12 cells (30). The mechanism by which Stx1A targets precisely to these clusters remains unclear. We have been able to identify the clusters of wild type Stx1A in living INS-1 cells employing TIRFM. For most of the mutants displayed in Fig. 1, we observed a homogenous distribution on the plasma mem-
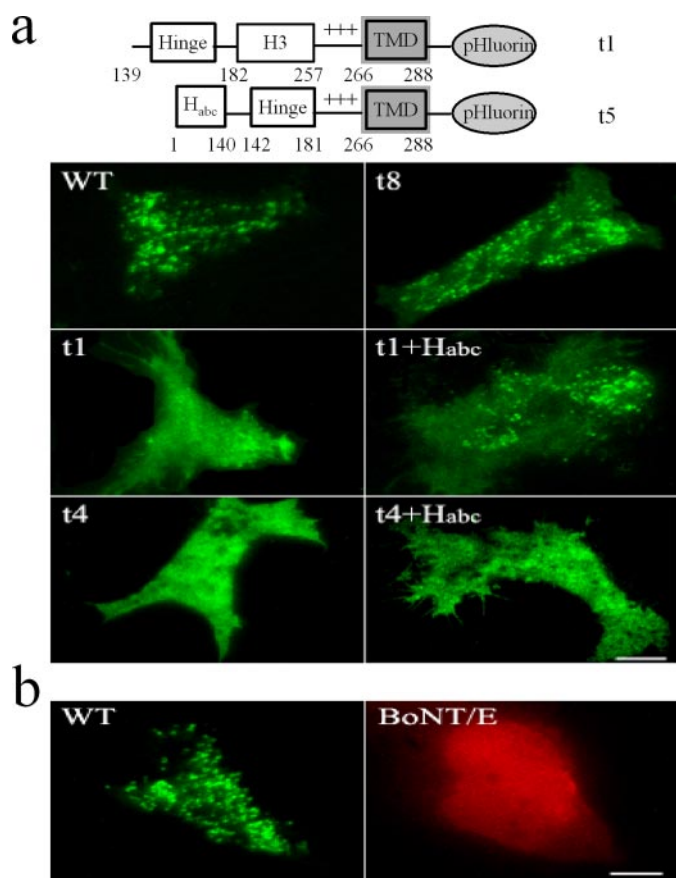
FIGURE 8. **H$_{abc}$ domain but not SNARE motif determines the cluster distribution at the fusion sites of Stx1A.** *a*, TIRFM images showing the clustering of Stx1A (wild type (*WT*)) and SNARE motif-truncated, but H$_{abc}$ domain-preserved mutant (t5), on the plasma membrane. Free H$_{abc}$ domain rescues the clustering of H$_{abc}$ domain-truncated mutants (t1 as an example). However, the lack of a half-SNARE motif abolishes the clustering of t4 even in the presence of free H$_{abc}$ domain. *b*, TIRFM image (*left*) of Stx1A (wild type (*WT*)) co-transfected with BoNT/E. The *right panel* is the wide field fluorescence image of mRFP from the same cell indicating the expression of BoNT/E. Treatment with BoNT/E cannot abolish the cluster distribution of Stx1A in INS-1 cells. *Bar*, 5 μm.

brane as exemplified by t1 in Fig. 8*a*. Only the t5 mutant that contains the intact H$_{abc}$ domain displayed a similar pattern of clustering as wild type. We verified that the t5 mutant co-localized with the wild type Stx1A (Stx1A-mOrange) in the clusters (data not shown) using dual-color TIRFM imaging. Interestingly, when the free H$_{abc}$ domain was co-expressed with those mutants, fluorescence clusters were detected in t1, t2, and t3 mutants (Fig. 8*a*). To verify whether free H$_{abc}$ domain interacts with SNARE motif and clusters these mutants, we further found that the t4 mutant with only half a SNARE motif could not form clusters in the presence of free H$_{abc}$ domain (Fig. 8*a*). It is plausible that free H$_{abc}$ domain complexes with H$_{abc}$-lacking Stx1A mutants that contain complete SNARE motif and then clusters these mutants together via either self-association or interaction with other proteins.

It has been proposed that the clustering of Stx1A could be due to its interaction with SNAP-25. In our hands, t5 mutant (lacking SNARE motif) expression leads to cluster distribution of fluorescence on the plasma membrane. This argues against a role of SNARE motif in targeting Stx1A to the cluster microdomain. In addition, we found that co-expression of BoNT/E could not abolish the clustering of Stx1A on the plasma membrane (Fig. 8*b*), further suggesting that the clustering of Stx1A is independent of the interaction with SNAP-25. Taken together, these results support a role for the H$_{abc}$ domain in targeting Stx1A to function sites.

DISCUSSION

Tail-anchored (or Type IV) membrane proteins constitute a class of integral membrane proteins that are held in the phospholipid bilayer by a single TMD close to the C terminus, while the entire functional N-terminal portion faces the cytosol. Examples of tailed-anchored proteins include syntaxin, VAMP-2 (28), Bcl-2 (31) family members, and so on, which play central roles in targeted membrane fusion or regulation of apoptosis, respectively. The function of these proteins is necessarily linked to its specific localization. Thus, understanding the targeting and insertion mechanisms of these proteins and the underlying regulation is an important issue with wide implications for cell biology. In this study, we have investigated the domain requirement for the trafficking and targeting of Stx1A, taking advantage of a method to quantify the faction of Stx1A at the plasma membrane. We have localized the minimal region necessary for the cell surface delivery of Stx1A to the C-terminal TMD and a few positive charged amino acids flanking the TMD. Although the long cytoplasmic domain of Stx1A may influence the final destination and trafficking efficiency of this protein (this study), our results propose that the plasma membrane delivery of Stx1A can be sufficiently determined by the summation of two factors: the TMD and the flanking positive charge. These two factors have also been suggested to be important for the targeting of other tail-anchored proteins (9).

Surprisingly, when the SNARE motif N-terminal to the minimal region existed, Stx1A mutants were retained in ER of CHO cells but were transported to the plasma membrane in INS-1 cells. We found that the membrane delivery of these SNARE motif-exposed Stx1A in INS-1 cells is mediated by the presence of endogenous SNAP-25, since cleavage of SNAP-25 with BoNT/E causes intracellular retention of the truncation. Recent work has demonstrated that Stx1A can assume two different conformations: a closed form, in which the H$_{abc}$ domain associates with H3 domain, and an open conformation, in which the association between these two domains is abolished (25, 32, 33). In the closed configuration, the N terminus of syntaxin folds over the SNARE motif and prevents its interaction with other SNARE proteins. To be able to interact with the cognate SNAREs, Stx1A must open first and expose the SNARE motif. However, we now show that inappropriate exposure of the SNARE motif at ER can cause ER retention, probably by nonspecific interaction with ER-resident SNARE proteins. Therefore, the SNARE motif of Stx1A must be covered during trafficking and only be exposed at the right sites and the right time. Apparently, the H$_{abc}$ domain is designed to fulfill this function.

It has been proposed that the trafficking of Stx1A may require interaction with other proteins. For instance, Munc18-1, a mammalian homologue of the *unc-18* gene, has been suggested to bind the closed form of Stx1A and transport Stx1A to the plasma membrane as a chaperone protein (10). Our data, however, do not support this hypothesis. First, we found in CHO cells, where no endogenous Munc18-1 has been found, that Stx1A is transported to the plasma membrane at a similar level as in INS-1 cells (Fig. 2). Is it possible that other ubiquitously expressed Munc18 isoforms participate in the trafficking of Stx1A in CHO cells? This is quite unlikely since those truncations lacking required domains for Munc18 interaction (33) are also translocated to the plasma membrane (Figs. 6 and 7). Furthermore, overexpression of Munc18-1 in CHO cells has no significant effect on the rate of Stx1A trafficking (Fig. 2*e*). Our results are consistent with the finding that syntaxin transportation to the cell surface is independent of UNC-18 protein in *C. elegans* (11) and Munc18-1 in mice (12). Together with our Munc18-1 knockdown experiment in INS-1 cells (Fig. 2*g*), these data hence support the conclusion that Munc18-1 is not required for the trafficking of Stx1A. The membrane delivery of SNARE motif-exposed Stx1A mutants, as shown in this study, involves the interaction with SNAP-

25. However, it is possible that the assembly of Stx1A and SNAP-25 in binary complex (28) will be non-productive, and hence SNARE motif-exposed Stx1A mutants will be trapped in a non-functional state.

To function appropriately, Stx1A must be correctly targeted to the specific sites of fusion at the plasma membrane. It has already been reported that Stx1A is concentrated in cholesterol-dependent clusters that define docking and fusion sites (30). However, factors defining the cluster distribution of Stx1A have not yet determined. Here we demonstrate that the H_{abc} domain is required for the clustering of Stx1A. Our data suggest that free H_{abc} domain can rescue the clustering of Stx1A mutants lacking H_{abc} domain, provided the presence of complete SNARE motif. Thus, it is possible that the H_{abc} domain of Stx1A interacts with other protein(s) in membrane microdomains to define the cluster distribution. It has been shown that Stx1A can directly bind and regulate the L-type Ca^{2+} channels (34, 35) in pancreatic β-cells. This led to the hypothesis that the H_{abc} domain could interact with Ca^{2+} channels and assure the spacial co-localization between Ca^{2+} influx and release sites. Further investigations will be necessary to find out the mechanism(s) that define the clustering sites of Stx1A.

In conclusion, the data presented here indicate that: 1) Stx1A is transported to the plasma membrane in both secretory INS-1 cells and nonsecretory CHO cells via its TMD spanned by a few positive charged amino acids; 2) exposure of the SNARE motif causes nonspecific retention in ER, which can be alleviated by the presence of SNAP-25; 3) the H_{abc} domain not only protects the SNARE motif from nonspecific interaction in the ER but also play a key role in targeting Stx1A to its sites of action after reaching the plasma membrane. This information will be helpful in further studies to understand how the function of Stx1A is precisely regulated at the precise sites of action.

REFERENCES

1. Hong, W. (2005) *Biochim. Biophys. Acta* **1744,** 120–144
2. Stojilkovic, S. S. (2005) *Trends Endocrinol. Metab.* **16,** 81–83
3. Ungar, D., and Hughson, F. M. (2003) *Annu. Rev. Cell Dev. Biol.* **19,** 493–517
4. Jahn, R., and Sudhof, T. C. (1999) *Annu. Rev. Biochem.* **68,** 863–911
5. Hay, J. C., and Scheller, R. H. (1997) *Curr. Opin. Cell Biol.* **9,** 505–512
6. Ferro-Novick, S., and Jahn, R. (1994) *Nature* **370,** 191–193
7. Broadie, K., Prokop, A., Bellen, H. J., O'Kane, C. J., Schulze, K. L., and Sweeney, S. T. (1995) *Neuron* **15,** 663–673
8. Saifee, O., Wei, L., and Nonet, M. L. (1998) *Mol. Biol. Cell* **9,** 1235–1252
9. Borgese, N., Colombo, S., and Pedrazzini, E. (2003) *J. Cell Biol.* **161,** 1013–1019
10. Rowe, J., Corradi, N., Malosio, M. L., Taverna, E., Halban, P., Meldolesi, J., and Rosa, P. (1999) *J. Cell Sci.* **112,** 1865–1877
11. Weimer, R. M., Richmond, J. E., Davis, W. S., Hadwiger, G., Nonet, M. L., and Jorgensen, E. M. (2003) *Nat. Neurosci.* **6,** 1023–1030
12. Toonen, R. F., de Vries, K. J., Zalm, R., Sudhof, T. C., and Verhage, M. (2005) *J. Neurochem.* **93,** 1393–1400
13. Zhang, W., Efanov, A., Yang, S. N., Fried, G., Kolare, S., Brown, H., Zaitsev, S., Berggren, P. O., and Meister, B. (2000) *J. Biol. Chem.* **275,** 41521–41527
14. Gonelle-Gispert, C., Costa, M., Takahashi, M., Sadoul, K., and Halban, P. (2002) *Biochem. J.* **368,** 223–232
15. Sanders, J. D., Yang, Y., and Liu, Y. (1998) *J. Neurosci. Res.* **53,** 670–676
16. Miesenbock, G., De Angelis, D. A., and Rothman, J. E. (1998) *Nature* **394,** 192–195
17. Yang, X., Xu, P., and Xu, T. (2005) *Biochem. Biophys. Res. Commun.* **330,** 914–920
18. Campbell, R. E., Tour, O., Palmer, A. E., Steinbach, P. A., Baird, G. S., Zacharias, D. A., and Tsien, R. Y. (2002) *Proc. Natl. Acad. Sci. U. S. A.* **99,** 7877–7882
19. Lomneth, R., Gimenez, J., Martin, T. F., and DasGupta, B. R. (1993) *Neuropharmacology* **32,** 285–289
20. Shaner, N. C., Campbell, R. E., Steinbach, P. A., Giepmans, B. N., Palmer, A. E., and Tsien, R. Y. (2004) *Nat. Biotechnol.* **22,** 1567–1572
21. Asfari, M., Janjic, D., Meda, P., Li, G., Halban, P. A., and Wollheim, C. B. (1992) *Endocrinology* **130,** 167–178
22. Miyagishi, M., Sumimoto, H., Miyoshi, H., Kawakami, Y., and Taira, K. (2004) *J. Gene Med.* **6,** 715–723
23. Mitchell, S. J., and Ryan, T. A. (2004) *J. Neurosci.* **24,** 4884–4888
24. Sankaranarayanan, S., De Angelis, D., Rothman, J. E., and Ryan, T. A. (2000) *Biophys. J.* **79,** 2199–2208
25. Yang, B., Steegmaier, M., Gonzalez, L. C., Jr., and Scheller, R. H. (2000) *J. Cell Biol.* **148,** 247–252
26. Loranger, S. S., and Linder, M. E. (2002) *J. Biol. Chem.* **277,** 34303–34309
27. Jahn, R. (2004) *Ann. N. Y. Acad. Sci.* **1014,** 170–178
28. Jahn, R., Lang, T., and Sudhof, T. C. (2003) *Cell* **112,** 519–533
29. Binz, T., Blasi, J., Yamasaki, S., Baumeister, A., Link, E., Sudhof, T. C., Jahn, R., and Niemann, H. (1994) *J. Biol. Chem.* **269,** 1617–1620
30. Lang, T., Bruns, D., Wenzel, D., Riedel, D., Holroyd, P., Thiele, C., and Jahn, R. (2001) *EMBO J.* **20,** 2202–2213
31. Cory, S., and Adams, J. M. (2002) *Nat. Rev. Cancer* **2,** 647–656
32. Dulubova, I., Sugita, S., Hill, S., Hosaka, M., Fernandez, I., Sudhof, T. C., and Rizo, J. (1999) *EMBO J.* **18,** 4372–4382
33. Misura, K. M., Scheller, R. H., and Weis, W. I. (2000) *Nature* **404,** 355–362
34. Lam, P. P., Leung, Y. M., Sheu, L., Ellis, J., Tsushima, R. G., Osborne, L. R., and Gaisano, H. Y. (2005) *Diabetes* **54,** 2744–2754
35. Yang, S. N., Larsson, O., Branstrom, R., Bertorello, A. M., Leibiger, B., Leibiger, I. B., Moede, T., Kohler, M., Meister, B., and Berggren, P. O. (1999) *Proc. Natl. Acad. Sci. U. S. A.* **96,** 10164–10169